



Combinatorial CAR design improves target restriction

Received for publication, October 9, 2020 Published, Papers in Press, November 24, 2020, <https://doi.org/10.1074/jbc.RA120.016234>

Hakan Köksal¹ , Pierre Dillard¹ , Asta Juzeniene² , Gunnar Kvalheim¹, Erlend B. Smeland^{3,4}, June H. Myklebust^{3,4} , Else Marit Inderberg¹ , and Sébastien Wälchli^{1,*}

From the ¹Department of Cellular Therapy, Department of Oncology, ²Department of Radiation Biology, Institute for Cancer Research, ³Department of Cancer Immunology, Institute for Cancer Research, Oslo University Hospital, Oslo, Norway; and ⁴K.G. Jebsen Centre for B Cell Malignancies, University of Oslo, Oslo, Norway

Edited by Peter Cresswell

CAR T cells targeting the B lymphocyte antigen CD19 have led to remarkable clinical results in B cell leukemia and lymphoma but eliminate all B lineage cells, leading to increased susceptibility to severe infections. As malignant B cells will express either immunoglobulin (Ig) light chain κ or λ , we designed a second-generation CAR targeting Ig κ , IGK CAR. This construct demonstrated high target specificity but displayed reduced efficacy in the presence of serum IgG. Since CD19 CAR is insensitive to serum IgG, we designed various combinatorial CAR constructs in order to maintain the CD19 CAR T cell efficacy, but with IGK CAR target selectivity. The Kz-19BB design, combining CD19 CAR containing a 4-1BB costimulatory domain with an IGK CAR containing a CD3zeta stimulatory domain, maintained the target specificity of IgK CAR and was resistant to the presence of soluble IgG. Our results demonstrate that a combinatorial CAR approach can improve target selectivity and efficacy.

Chimeric antigen receptors (CARs) are engineered molecules that enable T cells to recognize and eliminate antigen-positive target cells. The design of a CAR consists of the antigen recognition domain, usually derived from an antibody in which the variable fragments are arranged as a single-chain molecule (scFv) fused to different signaling domains (1). The first-generation CARs contain a single signaling domain derived from the CD3 zeta (CD3 ζ) protein, a crucial subunit of the CD3 complex that is involved in the early T cell receptor signaling, also known as signal 1. Owing to the cellular exhaustion resulting from the use of this signal domain only, CARs were reinforced with a costimulatory signaling domain such as 4-1BB and/or CD28 in later-generation constructs (a signal 2), which were then shown to improve proliferation and survival capacities of the CAR T cells (2, 3). It took 30 years for these molecules to be approved for clinical use, with the first therapeutic CAR target being CD19, a pan B cell antigen, thus expressed in B cell-derived lymphomas and leukemias (4, 5). Numerous clinical studies demonstrated significantly improved outcomes in relapsed and refractory B cell malignancies, and some of these studies were summarized in a recent review (6).

As a ubiquitous marker of B cells, CD19 was an ideal antigen to limit on-target off-tumor toxicity but nonetheless resulted in complete B cell aplasia (7–9). In a patient with follicular lymphoma, Kochenderfer *et al.* (10) demonstrated that complete B cell eradication, subsequent to CD19 CAR treatment, resulted in a drastic decrease of serum Ig with increased susceptibility to infection. The low levels of serum Ig were compensated for by frequent intravenous Ig supplements to treat infectious diseases.

The B cell receptor (BCR) is an attractive target as its expression is commonly maintained in malignant B cells (11). The BCR consists of two identical immunoglobulin (Ig) heavy and light chains, and owing to allelic exclusion of immunoglobulin (Ig) genes, malignant B cells from an individual tumor are clonal for their BCR and express either Ig kappa (κ) or Ig lambda (λ) light chains (12, 13). It was previously observed that genetic deficiency of the κ -chain, resulting in a complete absence of κ^+ IgG, did not prevent the patient from producing sufficient antibody titers to raise an immune response against infections (14). Thus, a κ^+ B cell aplasia can still be tolerable owing to the presence of λ^+ B cells. More than 10 years ago, an anti-Ig κ (IGK) CAR construct was shown to be efficient in preclinical models (12) and later tested in a phase I clinical trial (15). However, a major issue was that T cells redirected with IGK CAR, although potent, were shown to be sensitive to Ig in serum (12), suggesting that the manufacturing of the therapeutic CAR T cells in the presence of human serum (HS) might affect the quality and the potency of the cells before injection.

In this study, we aimed at developing an IGK CAR resistant to soluble IgG (sIgG), in order to enhance B cell malignancy treatment outcome by reducing CD19 CAR-related B cell aplasia. We reasoned that splitting the stimulatory signal 1 and 2 of the CAR into an "AND" combinatorial system would result in CAR T cells with improved properties. This strategy is based on prior studies, which have shown that a combinatorial approach could be used to enforce tumor specificity (16). We identified the Kz-19BB CAR design, combining IGK-CD3zeta (Kz) with CD19-4-1BB CAR (19BB) CAR, as an improved CAR. It is Ig κ restricted and resistant to sIgG. We further show that CAR T cells achieved optimal activation only when both antigens, CD19 and Ig κ , were present on the target cell, thus sparing the Ig λ^+ B cells. Hence, our combinatorial construct kept the advantages of both original CARs and in addition

This article contains [supporting information](#).

* For correspondence: Sébastien Wälchli, sebastw@rr-research.no.



Combinatorial IGK-CD19 CAR

overcame their weaknesses. Our data support future development of "AND system" designs that can exploit different surface targets with an expression that is not entirely restricted to cancerous cells.

Results

IGK CAR T cells specifically kill Igk⁺ target cells but are inhibited in the presence of human serum and soluble IgG

We designed a second-generation CAR by using the scFv from the anti-IGK hybridoma clone FN162 (Oslo University Hospital collection). To investigate the activity and specificity of the IGK CAR, we tested it against B cell lymphoma cell lines with variable Igk expression levels (REC-1, SU-DHL-4, BL-41, DAUDI, and U2932) and included three Igλ⁺ cell lines (Mino, Granta-519, MAVER-1), one cell line that lacked Ig light chains (SC-1) and two non-B cell controls (Jurkat and K562) (Fig. 1A and Fig. S1A). We assessed the specificity of our IGK CAR construct by testing the cytotoxic activity of primary human T cells transfected with IGK CAR mRNA toward different cell lines and demonstrated high specificity (Fig. 1B and Fig. S1B). As the activity of IGK CAR might be inhibited in the presence of serum Ig, we next tested IGK CAR-mediated killing of target cells in the presence of various dilutions of HS.

When comparing CD19 CAR and IGK CAR T cell efficacy against the Igk⁺/CD19⁺ target cell line BL-41, we observed that killing efficacy of IGK CAR, unlike CD19 CAR, was markedly reduced in the presence of HS (containing soluble IgG, IgA, and IgM), even at dilutions as low as 3.12% (Fig. 1C). This was further confirmed when purified sIgG (50 μg/ml) was added to the IGK CAR T cell/target cell coculture cytotoxicity assay, whereas the efficacy of CD19 CAR T cells remained unaltered (Fig. 1D).

Combinatorial design of IGK-CD19 CAR overcomes soluble IgG sensitivity

To overcome the reduced efficacy of IGK CAR T cells in the presence of HS while maintaining Igk target restriction, we designed different "AND"-type constructs of CD19 or Igk scFv using a single costimulatory domain, either 4-1BB domain (KBB and 19BB) or CD3ζ domain (Kz and 19z) (Fig. 2A). We first tested the expression efficiency of these constructs in T cells after transient transfection alone or in combination (19z-KBB and Kz-19BB). We used two different detection methods (anti-Fab and protein-L) since recognition sensitivity varied among constructs. The combinatorial CAR constructs demonstrated similar expression levels as the single CARs (Fig. 2B).

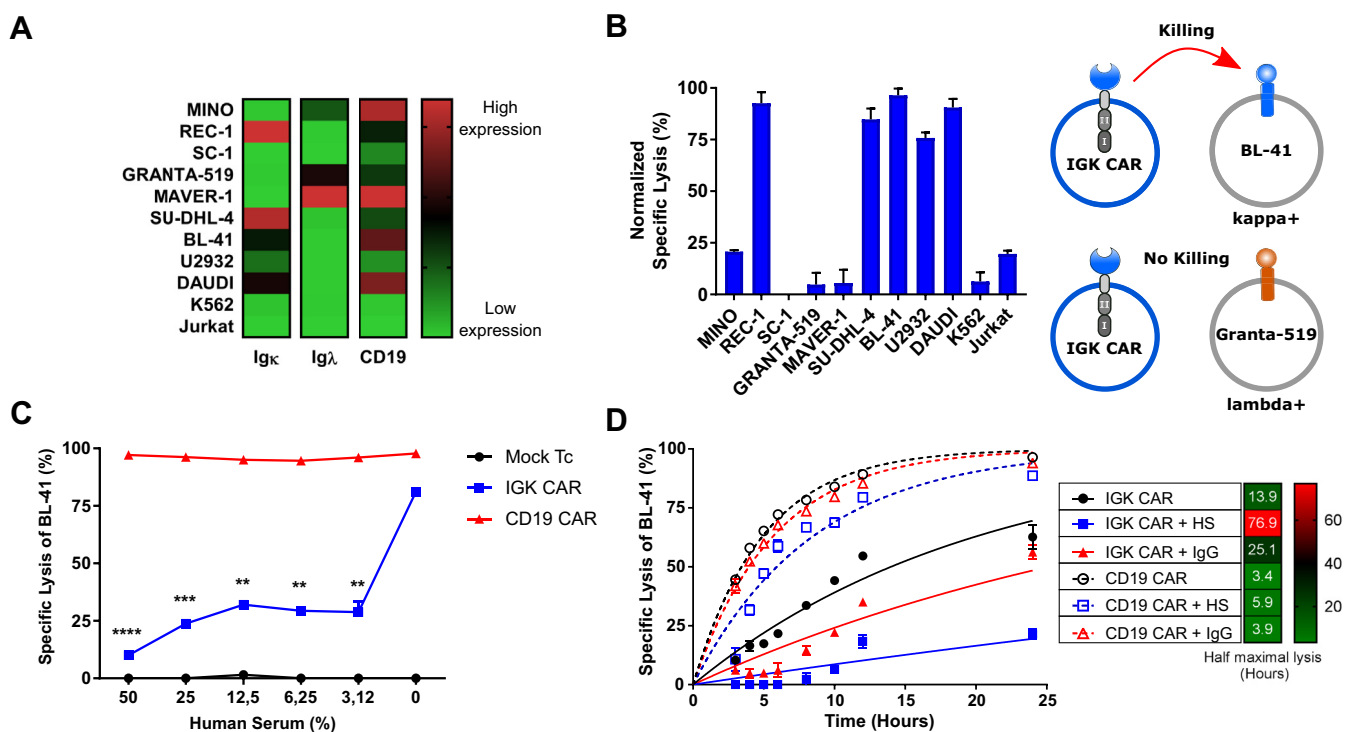


Figure 1. IGK chimeric antigen receptor (CAR) T cells target cancer cells specifically but are inhibited by human serum. A, flow cytometry analysis of Igk, Ig λ light chains, and CD19 expression on various cell lines. B, bioluminescence (BLI) killing assay of Mock T cells and IGK CAR T cells against various target cells (25:1 E:T ratio). Shown is specific lysis as normalized values relative to Mock T cells after 6 h of coculture. Representative data from one of two independent experiments are shown. Data represent mean ± SD of quadruplicates. C, BLI killing assay of Mock T cells, CD19 CAR- and IGK CAR-transfected T cells cocultured with Igk⁺ BL-41 lymphoma cell line for 10 h (10:1 E:T ratio) in the presence of increasing human serum concentration. Data represent mean ± SD of triplicates. Representative data from one of two independent experiments are shown. D, BLI killing assay of CD19 CAR- and IGK CAR-transfected T cells cocultured with BL-41 cell line for 24 h (10:1 E:T ratio) in the presence of 50% human serum or 50 μg/ml of IgG. Half maximal lysis was obtained via one phase exponential fitting. Data represent mean ± SD of triplicates. Representative data from one of two experiments are shown. ***p* < 0.01, ****p* < 0.001, *****p* < 0.0001

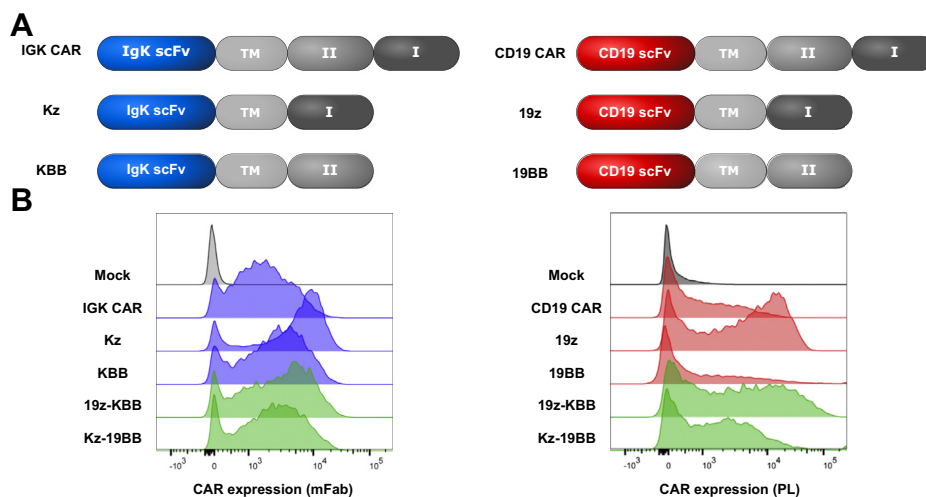


Figure 2. Design and expression of the classic and combinatorial chimeric antigen receptor (CAR) constructs. *A*, schematic representation of all classic and combinatorial CAR constructs. TM, CD8a transmembrane; I, CD3 ζ ; II, 4-1BB. *B*, Ig κ and CD19 single chain variable fragment–based mRNA constructs were electroporated into primary T cells. Ig κ and CD19–redirected CAR expression was measured by staining with anti-mouse Fab and protein L, respectively. Representative fluorescence-activated cell sorting analysis of T cells 18 h after electroporation is shown.

To test if the combinatorial CAR T cells could overcome inactivation by sIgG, we monitored the cytolytic activity of the different constructs against Ig λ -/Ig κ + /CD19+ BL-41 cells in the presence or absence of sIgG (Fig. S2A). As shown in Figure 3A, the IGK CAR T cells were sensitive to the presence of sIgG, whereas the Kz-19BB construct was insensitive. This suggests that the efficacy of CAR T cells was primarily regulated by the CD3 ζ domain–linked scFv and that the 4-1BB costimulatory domain by itself was not sufficient to induce significant cytotoxic activity. Furthermore, as expected, we did not observe any effect of sIgG when Granta-519 cells (Ig λ + /Ig κ - /CD19+) were targeted (Fig. 3B), supporting that Kz-19BB CAR had primarily acquired IGK CAR selectivity. All constructs alone or in combination were tested and confirmed that the 19z-KBB CAR T construct followed CD19 CAR selectivity (Fig. S2, A–B). These data further suggest that the Kz-19BB construct provided resistance to sIgG and confer the IGK CAR selectivity to Ig κ + cells. In order to quantify the sIgG inhibition, we also ran a killing assay with titrated soluble sIgG in the medium for all constructs, again demonstrating that Kz-19BB had acquired an advantage over IGK CAR (Fig. 3C and Fig. S2C).

We next analyzed cytokine production in the same conditions, where IGK CAR and Kz-19BB showed a reduced cytokine production compared with CD19 CAR–expressing CD8 T cells in response to BL-41 cells but were not sensitive to sIgG (Fig. 3, D–G). The difference in sensitivity to sIgG in the two assays was probably due to the longer kinetics for cytokine response. These data were confirmed when all the constructs were run in combination or alone, with the exception of Kz alone being sensitive to sIgG in CD8 T cells (Figs. S2, D–G) and CD4 T cells (Fig. S3, A–D). This increased sensitivity could be due to the absence of a secondary costimulatory signal. As cytokine release was not affected by sIgG in our setting, these data confirm that selectivity of combinatorial

constructs followed the identity of the CD3 ζ domain–carrying chain.

Kz-19BB offers a trade-off between specificity and IgG insensitivity

We next studied the impact of the 19BB construct density on the cytotoxicity and on the IgG sensitivity of the Kz-19BB CAR (Fig. 4 and Fig. S4), using different concentrations of mRNA for electroporation to fine tune the surface density of the 19BB CAR constructs. First, we determined the baseline cytotoxic activity by Mock T cells with little to no activity (Fig. 4A). Then, we determined the baseline for IgG or HS sensitivity by IGK CAR and Kz, which demonstrated substantial inhibition rates (Fig. 4, B–C). However, the inhibition by serum or soluble Igs (sIg) was drastically decreased when Kz and 19BB were combined at a ratio of 1 to 0.5 (Kz-19BBx0.5) (Fig. 4D). At equimolar expression of Kz and 19BB or at increased concentrations of 19BB (Kz-19BBx2), the CAR T cell–mediated lysis of Ig κ + /CD19+ BL41 target cells was even faster than with CD19 CAR and demonstrated potent killing even in the presence of IgG and HS (Fig. 4, E–H). On the other hand, the same CAR T cells showed 19BB density-dependent cytotoxicity against Ig λ + /CD19+ Granta-519 cells. Hence, a higher 19BB concentration leads to a higher cytotoxic response toward the Granta-519 cell line (Fig. S4, A–F). Even at the highest concentration of 19BB, the cytotoxic efficiency of combinatorial CARs against the Ig κ - Granta-519 cell line was lower than that of CD19 CAR, demonstrating the conserved specificity to Ig κ -expressing targets of combined CARs (Fig. S4, F–H). Furthermore, this suggests a correlation between the density of the 19BB construct and the resistance to IgG inhibition, with specificity as a trade-off, which is in line with previous studies, suggesting that the costimulatory signal improves the phosphorylation kinetics of the T cell receptor signaling and boosts the response (17).

Combinatorial IGK-CD19 CAR

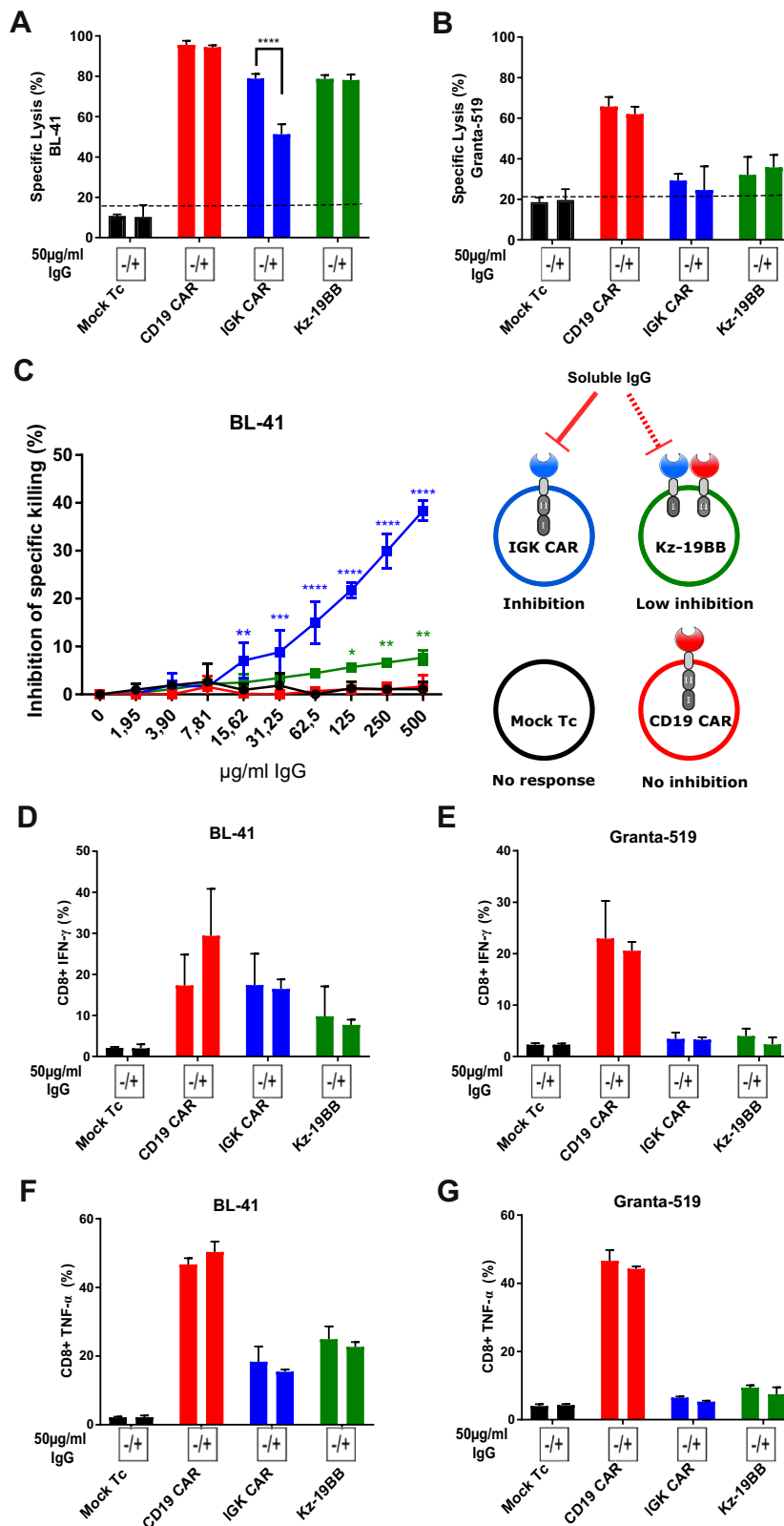


Figure 3. Combinatorial chimeric antigen receptor (CAR) T cells are less sensitive to serum inhibition while maintaining specificity. A–B, bioluminescence killing assay of Mock T cells and CAR construct–electroporated T cells cocultured with Igk⁺ BL-41 or Igk⁻ Granta-519 cell lines for 10 h (10:1 E:T ratio) in the presence or absence of serum purified IgG (50 µg/ml). Data represent mean ± SD of quadruplicates. Representative data from one of three independent experiments are shown. C, bioluminescence killing assay of Mock T cells and CAR construct–electroporated T cells cocultured with BL-41 cell line for 10 h in the presence of an increasing concentration of IgG (10:1 E:T ratio). Specific lysis inhibition corresponds to the difference of cytotoxic capacity of each construct between IgG+ and IgG– conditions. Data represent mean ± SD of triplicates. One-way ANOVA was performed between Mock T cell and other groups for each IgG concentration. D–G, CD8+ T cell intracellular cytokine staining (IFN-γ and TNF-α) after cocultivation with BL-41 or Granta-519 cell lines in the presence or absence of IgG at 50 µg/ml (for 24 h, 1:2 E:T ratio) Data represent mean ± SD of triplicates. Representative data from one of two independent experiments are shown. A, B, D–G, significance was assessed by Student's *t* test comparing IgG+ and IgG– conditions. **p* < 0.05, ***p* < 0.01, ****p* < 0.001, *****p* < 0.0001.

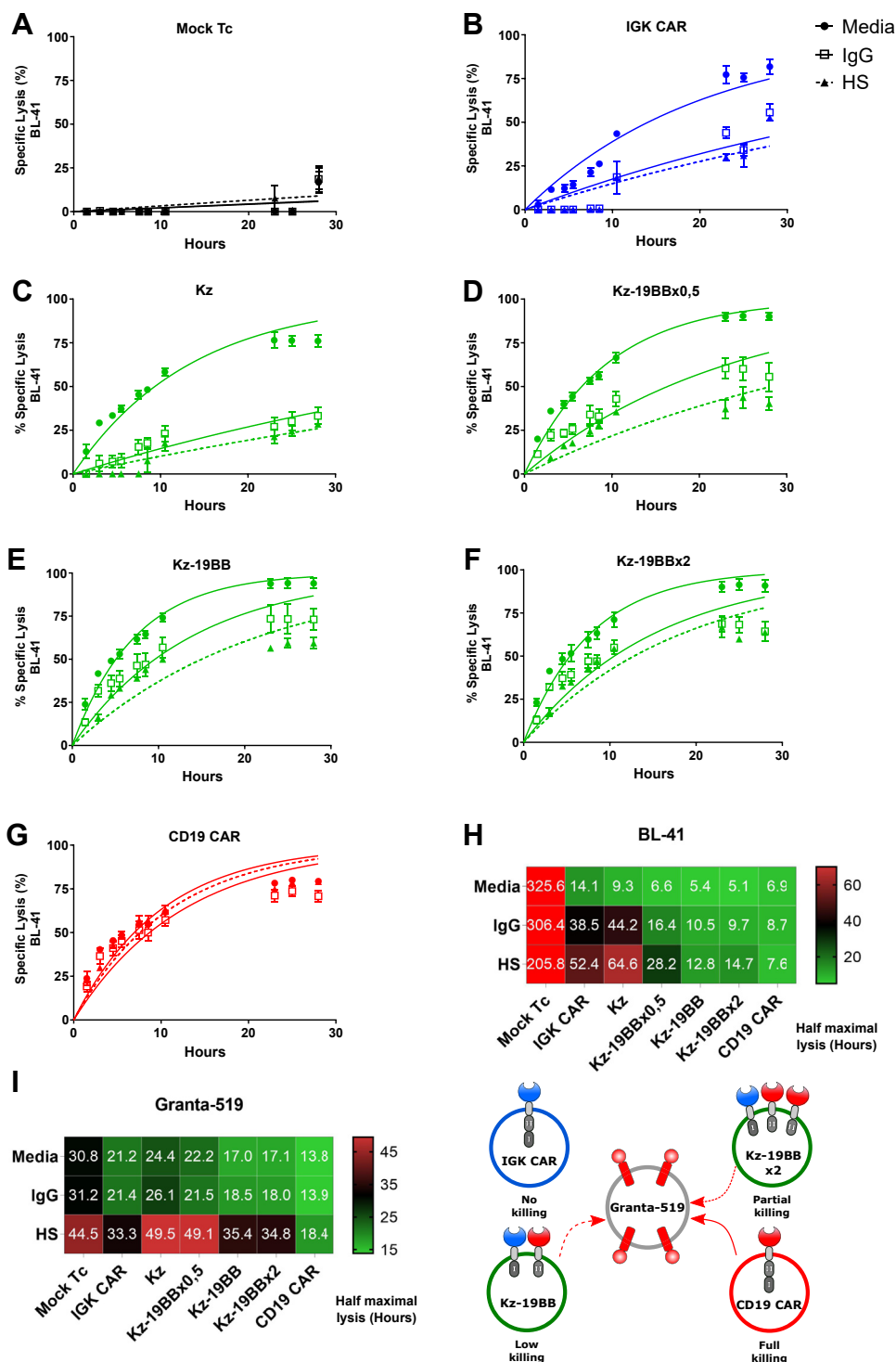


Figure 4. Kz-19BB offers a trade-off between IgG insensitivity and Igk specificity. A–G, BLI killing assay of Mock-electroporated and CAR construct-electroporated T cells cocultured with BL-41 or Granta-519 target cell lines in assay media, 50% human serum, or 50 µg/ml IgG (10:1 E:T ratio). The Kz-19BB construct was prepared with varying concentrations of the 19BB part. Representative results only include analyses against the BL-41 cell line. *H–I*, heat maps of half maximal lysis values obtained *via* one phase exponential fitting. Data represent mean ± SD of quadruplicates. Representative data from one of three experiments are shown.

Kz-19BB conserves IGK CAR characteristics

To compare molecular and physiological characteristics of T cells expressing the combinatorial CARs, we monitored T cells electroporated with CAR constructs upon stimulation with

surface-coated antibodies where IgG was used as an Igk-specific stimulant and anti-CD3 as a general stimulant, independently of CAR specificity. Only IGK CAR and Kz-19BB T cells increased their metabolism (respiration capacity) upon

Combinatorial IGK-CD19 CAR

incubation on an IgG-coated surface, exhibiting a state of immune activation. As expected, the same metabolic pattern and level of stimulation were observed when T cells were incubated on the anti-CD3 coated surface (Fig. S5, A–C). In agreement with our previous data, 19z-KBB-expressing T cells were not stimulated by IgG coating. We then studied the early signaling profile generated by the combined construct compared with the original ones. The activation profile of Kz-19BB CAR was measured by time-lapse imaging of ZAP-70 kinase phosphorylation (Fig. S5D). A synthetic surface was obtained after glass coating of IgG, anti-CD3, or poly-L-lysine. Similar to IGK CAR T cells, the combinatorial Kz-19BB CAR T cells were responsive to IgG and anti-CD3 coating by transient phosphorylation of ZAP-70 kinase. In contrast, CD19 CAR showed only anti-CD3-induced phosphorylation (Fig. S5E). These results were confirmed by measuring the density of adhered cells per unit of area, a direct measurement of T cell activation (Fig. S5F). Taken together, these results demonstrated a comparable activation phenotype of Kz-19BB and IGK CAR cells upon Ig-kappa target.

Impact of sIgG on Igk targeting CAR T cells

We next studied if sIgG had an effect on CAR T cell expansion. In order to use a system close to common clinical manufacturing, we employed a retroviral expression system and designed a combinatorial retroviral construct where Kz and 19BB were separated by a 2A ribosome skipping sequence, which guarantees a close to equimolar production of the two CARs (18). Three separated constructs encoding IGK CAR, Kz-19BB CAR, and CD19 CAR were prepared (Fig. 5A) and expressed in T cells (Fig. 5B). These cells were expanded into two separate cultures either with HS or with serum replacement (SR) for 11 days, and the cell number, the viability, and the level of CAR expressions were monitored. Overall, T cells expanded more efficiently in HS than in SR. We also observed that IGK CAR T cells were slightly less confluent than all other

HS-expanded T cells (Fig. 5, C–D), which could be reminiscent of this constant stimulation of the receptor by sIgG. We next analyzed the cell viability and, in agreement with previous observations, noticed that HS-expanded cells overall led to more viable cells than SR-expanded cells and detected no difference between IGK CAR and Kz-19BB-expressing T cells (Fig. S6A). To investigate the general trend, we divided SR values over HS (Fig. S6B). Finally, the expression of IGK CAR and Kz-19BB T cells was decreased when expanded in HS, whereas CD19 CAR T cells were not affected (Fig. S6, C–F); thus, Kz-19BB could not counteract the sIgG effect after long-term stimulation. Again, this effect was probably linked to a constitutive recycling of a stimulated receptor. Of importance, although the percentage of CAR expression was not dramatically affected (Fig. S6, C–D), the intensity of CAR expression was decreased by threefold at the end of the expansion (Fig. S6, E–F). In line with these observations, we were able to detect that IGK CAR and Kz-19BB were stimulated and expanded by incubation with soluble or coated IgG (Fig. S7, A–B). These last data are in agreement with studies showing the stimulating effect of dimeric soluble factors on CAR T cells (19). Together, these data point toward a mild improvement of Kz-19BB over IGK CAR in HS-containing culture medium, in terms of cell number. However, the loss of CAR expression and the viability could not be completely overcome.

Stable Kz-19BB-expressing T cells demonstrate IGK CAR selectivity

We then tested whether a stable equimolar expression maintained Igk selectivity. Specificity and cytotoxic capacities of the transduced T cells were assessed in a bioluminescence assay against BL-41 and Granta-519 cell lines, with similar results to what was observed upon mRNA electroporation (Fig. 6, A–B). However, this statement might not apply to a situation of high CAR expression or saturated antigen density (see discussion). We further verified the selectivity of Kz-19BB

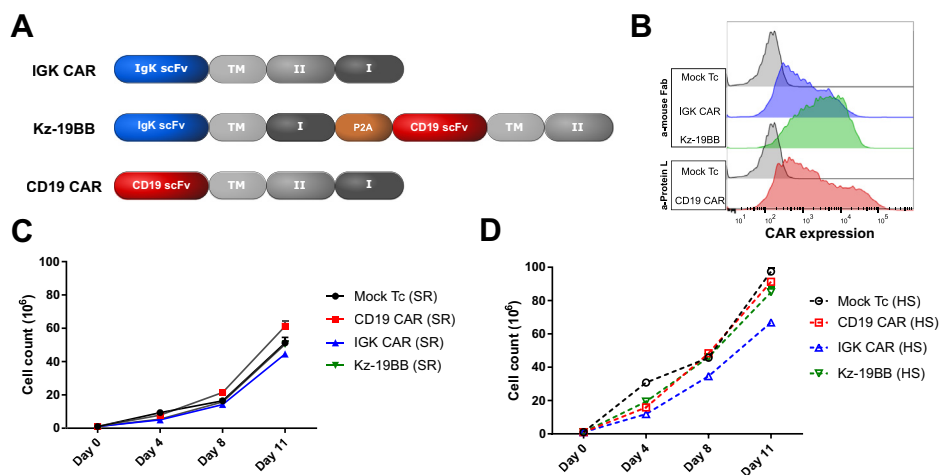


Figure 5. Impact of human serum on stable IGK chimeric antigen receptor (CAR)-expressing T cell expansion. A, schematic representation of Kz-19BB, IGK, and CD19 CAR constructs. B, CAR expressions were analyzed after transduction and 11 days expansion of primary T cells by staining with anti-mouse Fab or Protein L antibody. C–D, Mock and CAR-expressing T cells were expanded in either SR (serum replacement) or HS (human serum) containing X-VIVO-15 complete medium for 11 days. Cell counts were evaluated on days 0, 4, 8, and 11 by a Countess cell counter utilizing trypan blue exclusion.

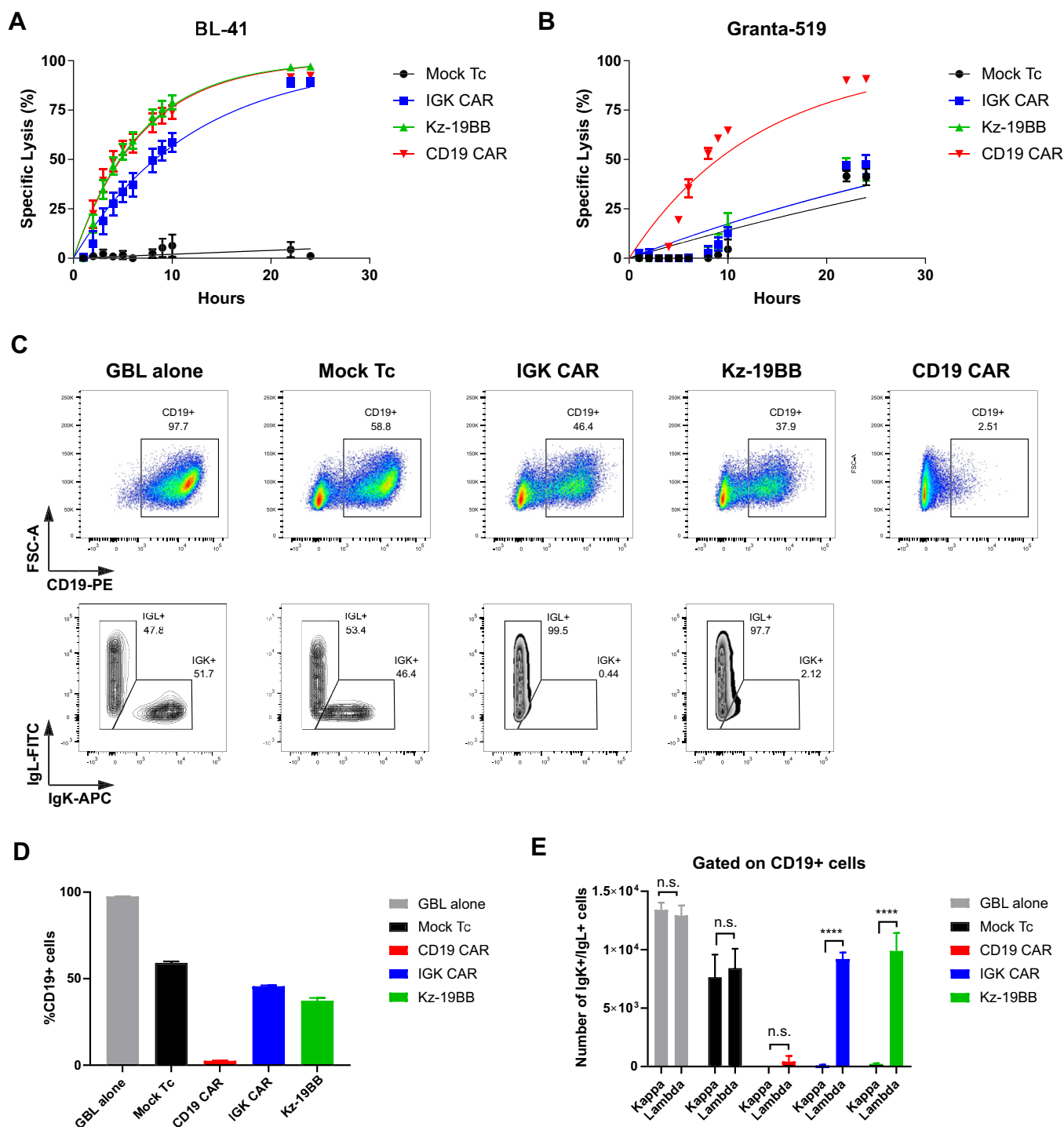


Figure 6. Kz-19BB is efficient when stably expressed and demonstrates similar specificity against mixed cell cultures. A–B, bioluminescence killing assay of Mock and CAR-transduced T cells cocultured with BL-41 or Granta-519 target cell lines (10:1 E:T ratio). Data represent mean \pm SD of triplicates. Representative data from one of two experiments are shown. C–E, retrovirally transduced T cells cocultured for 12 h with both BL-41 and Granta-519 target cell lines at a ratio of 2:1:1, respectively. After coculture cells were stained with anti-CD19-PE, anti-Igk APC, and anti-Ig λ -FITC. Data represent mean \pm SD of quadruplicates. Data pooled from two independent experiments. **** p < 0.0001, n.s. not significant.

CAR in a mixture of target cells (Igk+ and Igk-). As shown, unlike CD19 CAR T cells, IGK CAR and Kz-19BB CAR T cells selectively killed Igk+/CD19+ BL-41 cells but not Igk-/CD19+ Granta-519 (Fig. 6, C–E). We confirmed these observations using Epstein Barr virus (EBV)-transformed primary B cells cocultured with IGK and Kz-19BB CAR T cells and

demonstrated that Igk+ EBV+ B cells were specifically eliminated, whereas CD19 CAR eliminated all B cells (Fig. S8, A–C). We finally confirmed the target restriction of our construct by including an osteosarcoma cell line OHS (CD19-/Igk-) (Fig. S8, D–E). These data suggest that the scFv linked to the CD3 ζ domain determined the target selectivity, whereas the

Combinatorial IGK-CD19 CAR

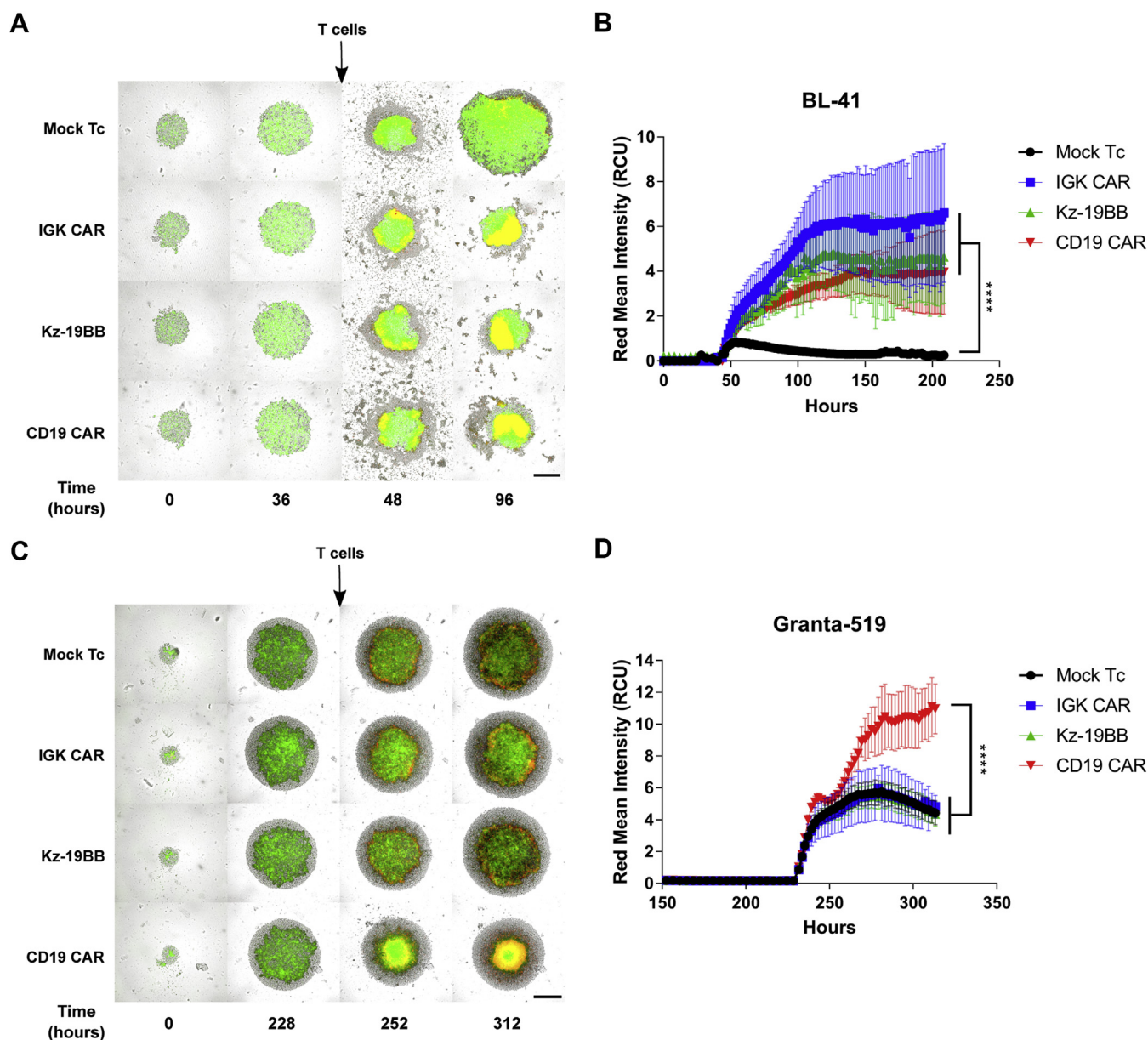


Figure 7. Kz-19BB is efficient when stably expressed and demonstrates similar specific potency against 3D tumor cultures. A and C, representative micrographs of BL-41 and Granta-519 spheroids, respectively, cocultured with either Mock, IGK CAR-, Kz-19BB-, or CD19 CAR-expressing T cells. Both cell lines are GFP/Luc+. Red signal represents the presence of annexin V. The scale bars represent 400 μ m. B and D, annexin V measurements of spheroids over time. Data represent means \pm SD of hexaplicates. Representative data from one of two independent experiments are shown. Two-way ANOVA test was performed to compare groups. **** $p < 0.0001$.

scFv linked to the 4-1BB domain could potentiate the efficacy of the T cells upon expression of the combinatorial CAR.

Kz-19BB is efficient against 3D tumor spheroids

We finally assessed the efficacy of Kz-19BB against 3D spheroid tumors and compared it with the performance of the single CARs. We established 3D lymphoma spheroids to analyze the efficacy and specificity of Kz-19BB against tumor formations that are related to *in vivo* structures. To this end, BL-41 and Granta-519 spheroids were prepared on agar-coated wells. T cells were added when spheroid diameters were around 1 μ m. The annexin V substrate was used to

monitor apoptosis by live cell imaging. In agreement with the killing assays, BL-41 spheroids were lysed by all CAR T cells (Fig. 7, A–B), whereas only CD19 CAR T cells demonstrated significant impairment of Granta-519 spheroid growth (Fig. 7, C–D). Together these data confirm that the combinatorial Kz-19BB CAR construct was as efficient and selective as the original second-generation IGK CAR in controlling tumor growth in a complex tumor structure.

Discussion

CD19 CAR T cell therapy has shown remarkable clinical efficacy in multiple subtypes of B cell lymphoma (20) and led

to the US Food and Drug Administration approval of two CD19 CAR products for relapsed or refractory B-cell acute lymphoblastic leukemia and aggressive non-Hodgkin lymphoma treatment (21–24). However, this treatment comes with a critical pitfall: by directing T cells toward the CD19 antigen, a common lineage marker, the entire B cell population is indiscriminately eradicated, which in turn impairs patients' humoral immune response (11). There is therefore a need for alternative target antigens with less off-tumor toxicity. To this end, we and others (12) selected a restricted lineage marker, the Ig κ light chain of the BCR. The clonal light chain expression on most B-NHL subtypes makes this an ideal therapeutic target to limit on-target, off-tumor toxicity. Despite some objective responses demonstrated after treatment with IGK CAR in a phase I clinical trial (15) where the impact of soluble Ig κ was discussed, no data showing the resistance to sIgG were presented. We reasoned that, despite its serum sensitivity, IGK CAR could improve the CD19 CAR construct selectivity in a combinatorial "AND" format (16). Since this format requires splitting of the signaling unit, T cell sensitivity to serum would be attenuated owing to the lack of costimulation provided by the CD19 CAR in the presence of serum proteins.

The initial evaluation of our IGK CAR demonstrated that it was potent and specific but sensitive to HS and sIg, thus in agreement with previous reports (12). We combined IGK CAR and CD19 CAR with different signaling domains and confirmed previous reports showing that the CD3 ζ domain (ζ) was the major driver of the CAR T cell activation determining the specificity of the construct. As expected, the costimulatory domain 4-1BB (BB) was not able to trigger a significant CAR-mediated T cell killing by itself but could be exploited to attenuate serum sensitivity. Indeed, even if the adjunction of the 19BB construct to the Kz part did not boost the activation, it drastically reduced the inhibition caused by HS. Further analyses of the Kz-19BB combination demonstrated similarity with IGK CAR in terms of specificity and activation (in response to IgG or Ig κ ligand binding). For these experiments, we used mRNA coelectroporation to adjust individual components and hence control the protein levels. Besides flexibility regarding specificity and sensitivity toward IgG inhibition, the mRNA concentration had a major impact on the functional outcome. This was in line with a recent publication demonstrating that a two-output biological circuit can be pushed in one direction or the other by altering mRNA concentrations alone (25). Accordingly, we used varying concentrations of the 19BB part and observed that the design could be even more intricate and flexible than intended. Each increasing concentration of 19BB yielded a CAR construct less sensitive to IgG inhibition, but with specificity closer to that of CD19 CAR, allowing us to control the trade-off. This concept provides additional advantages such as the interchangeability of the 4-1BB linked parts. As an example, in the case of CD19 negative relapse, one could use an alternative targeting scFv, such as CD22 (26) or CD37 (27, 28) to overcome the loss of CD19.

We also assessed the efficacy and specificity in retroviral settings. Including a P2A ribosomal skipping sequence allowed us to have an equimolar expression of Kz and 19BB parts. During the expansion comparison of the T cells, we observed that HS provides a better T cell environment leading to higher expansion rates and higher viabilities than SR. Although a slight benefit of Kz-19BB was detected in the cell number after 11 days of expansion, both IGK and Kz-19BB CAR T cells demonstrated lower CAR expression in HS. This suggests that both activation antibodies and serum components in the media overstimulate the IGK and Kz-19BB constructs leading to elimination of high-intensity CAR-expressing T cells or important recycling. Thus, the combinatorial CAR, although efficient in maintaining selective killing, was not able to overcome the negative effect of the sIgG on the CAR T cells. It is tempting to speculate that this was due to normal receptor recycling upon ligand binding, but whether this will impact the final clinical product will need to be evaluated. Nevertheless, this issue is manageable; one could use either SR instead of HS or alternative T cell media that do not require serum supplementation (29).

In order to proceed with the evaluation of Kz-19BB, we performed 3D tumor spheroid killing assays because they mimic some of the *in vivo* tumor properties (30, 31). Despite the expansion downsides, both IGK CAR and Kz-19BB still demonstrated significant cytotoxicity against BL-41 spheroids and maintained their selectivity against Granta-519 spheroids.

The construct presented herein is a prototype, and alternative versions will be designed in which the affinity of one of the scFv can be modified: it is tempting to speculate that a lower-affinity CD19 CAR (32) would reduce the recognition of Ig λ + / CD19+ targets. A similar observation was also noted with our high-affinity anti-Ig λ (IGL) CAR (33) when designed in a CD19-combinatorial construct (unpublished data). Another possible improvement would be the regulation of the expression: a lower or controlled presence of the construct could also affect the Ig λ + / CD19+ target recognition as supported by our mRNA titration studies, where the increased IGK part reduced CD19 CAR dominancy. To overcome the variable CAR expression, one could CRISPR guide the combinatorial CAR to have a predictable and comparable expression level in each transduction (34).

In summary, we describe an alternative CD19 CAR, which becomes selective through IGK combination to avoid B cell aplasia. One can predict that this format will be used to combine alternative targets, thus improving selectivity, which should result in an increased safety.

Experimental procedures

Plasmid design

A DNA sequence encoding the anti-Ig κ scFv was generated after sequencing the original hybridoma (FN162). Briefly, the sequences of the VL and VH regions were determined by 5'-RACE (33). The design consists in the linkage of the two chains with a (G₄S)₄ linker. Synthetic sequences were acquired

Combinatorial IGK-CD19 CAR

at Eurofins MWG (Ebesberg Germany). The scFv for the CD19 CAR (fmc63 clone) was a kind gift from Martin Pule (University College London, UK) that we subcloned in our codon-optimized second-generation signaling tail, which is composed of a CD8 hinge and transmembrane domain linked to 4-1BB and CD3 ζ . The scFvs and the signaling tail were subcloned into pENTR Gateway (Thermo Fisher, Waltham, MA, USA) and further subcloned in compatible expression vectors (35). Combinatorial CAR clonings were performed by modified CAR tails. The constructs containing only 4-1BB were prepared by introducing a stop codon *via* site-directed mutagenesis after the 4-1BB domain with the following primers (5'-3'): forward GGTTGTGAGCTGTGAGTGAAGTTTTCC, reverse GGAA AACTTCACTCACAGCTCA CAACC. The constructs with only the CD3 ζ tail were synthesized by Eurofins-MWG and fused to the scFv sequences. To clone the Kz-2A-19BB construct for retroviral expression, the sequence coding for a partial site from the end of Igk scFv and rest of the CAR tail, P2A ribosome skipping sequence (18), and partially the beginning of the CD19 scFv sequence were synthesized by Eurofins-MWG. The ligation of different elements of the final construct was performed into a pENTR vector. The firefly luciferase-GFP fusion protein coding sequence (a kind gift from Rainer Löw, EUFETS AG, Germany) (36) was incorporated into pMP71 and used to stably transduce target cell lines as reported in (37).

Cell lines, media

The human cell lines, BL-41, GRANTA-519, DAUDI, REC-1, SU-DHL-4, U2932, SC-1, MINO, K562, and MAVER-1 were obtained from DSMZ. J76 was a kind gift from M. Heemskerk (Leiden University Medical Center, the Netherlands). EBV-transformed B cell lines were generated in house. The cells were cultured in RPMI 1640 (PAA, Pasching, Austria) and supplemented with 10% fetal calf serum (FCS, PAA) and 50 μ g/ml Gentamycin (Thermo Fisher, Oslo, Norway). The Phoenix-AMPHO (CRL-3213) cell line was purchased from ATCC (Manassas, VA, USA) and was maintained in Dulbecco's modified Eagle's medium (Sigma-Aldrich, Oslo, Norway) supplemented with 10% FCS and 50 μ g/ml Gentamycin.

Soluble IgG purification

sIgG was purified directly from HS using Pierce Protein A/G Agarose (Thermo Fisher Scientific) by following the manufacturer's protocol. In brief, first, the Protein A/G agarose was loaded on Micro Bio-Spin Chromatography Columns (Bio-Rad Laboratories, Hercules, CA, USA). After gravity flow, HS was loaded. sIgG was eluted from the agarose by 0.1 M glycine pH 2, then neutralized by 1 M Tris pH 8. The concentration of purified IgG was measured on Nanodrop (Thermo Fisher Scientific).

Synthetic mRNA preparation

In vitro transcribed (IVT) mRNA was synthesized using RiboMAX T7 Kit (Promega, Madison, WI, USA) as described (37, 38). Anti-Reverse Cap Analog (ARCA, Trilink Biotechnologies, San Diego, CA, USA) was used for mRNA

capping. The IVT mRNAs were evaluated by agarose gel electrophoresis and Nanodrop (Thermo Fisher Scientific, Waltham, MA, USA) for quality and quantity, respectively.

In vitro expansion of human T cells

Human peripheral blood mononuclear cells (PBMCs) were isolated from healthy donors by a protocol adapted from T cell production under GMP conditions as described (39). In brief, PBMCs were separated from blood by density gradient and cultured in the presence of Dynabeads (Dynabeads *ClinExVivo* CD3/CD28, Thermo Fisher, Oslo, Norway) in X-VIVO 15 (Lonza, Basel, Switzerland) supplemented with 100 U/ml recombinant human IL-2 (Proleukin, Prometheus Laboratories Inc, San Diego, CA, USA) and 5% HS for 11 days. When specifically mentioned, CTS SR (Thermo Fisher Scientific) was used instead of HS. On specific days, a small volume of media was separated from the culture and subjected to Countess II Automated Cell Counter (Thermo Fisher Scientific) to monitor viability and numbers during the expansion phase. Expanded T cells were frozen in batches and stored in liquid nitrogen for future manipulation.

IVT mRNA electroporation of human T cells

Expanded T cells were washed twice with nonsupplemented RPMI media and resuspended at 70×10^6 cells/ml. The IVT mRNA was mixed with the washed T cells at a concentration of 100 μ g/ml. The mix was transferred to a 4-mm cuvette and electroporated at 500 V and 2 ms using a BTX 830 Square Wave Electroporator (BTX Technologies Inc, Hawthorne, CA, USA). After electroporation, T cells were transferred to complete culture medium and then left at 37 °C in 5% CO₂ overnight. In coelectroporation cases, the total concentration of IVT mRNA for each construct was halved. In IVT mRNA titration case, the total mRNA concentration was maintained by an irrelevant GFP coding mRNA.

Retroviral transduction of human T cells

Retroviral supernatants were collected as described (25). PBMCs were isolated from healthy donors as described above. After isolation, PBMCs were resuspended in complete X-VIVO 15 medium and transferred to a 24-well plate coated with anti-CD3 (1 μ g/ml, OKT clone, Thermo Fisher, Norway) and anti-CD28 (1 μ g/ml, CD28.6 clone, Thermo Fisher, Norway) at 1×10^6 cells/well. Cells were then left at 37 °C in 5% CO₂ for 3 days. Activated T cells were transferred to another 24-well plate (Nunc A/S, Roskilde, Denmark), pre-coated with retronectin (50 μ g/ml, Takara Bio, Inc, Shiga, Japan). Activated T cells were spinoculated at 32 °C at 750g for 60 min. The spinoculation was repeated once more the following day with fresh medium and retroviral supernatant. Afterward, T cells were washed twice with complete X-VIVO 15 culture medium, transferred to a new 24-well plate and maintained in culture for transduction efficiency assessment. Transduced T cells were expanded with anti-CD3/28 Dynabeads as described earlier. Expanded T cells were frozen in aliquots and transferred to liquid nitrogen for future use.

Functional assay and flow cytometry

Expression validations were done by flow cytometry. Cell lines or primary cells were washed twice with flow buffer (PBS with 2% FCS). Cells were then resuspended in antibody-containing flow buffer for 15 min at room temperature and washed twice with the flow buffer. Validation of CAR expression was performed with two antibodies. All CAR combinations with anti-Ig κ scFv were assessed with anti-mouse Fab (Biotin-SP (long spacer) AffiniPure F(ab')₂ Fragment, Jackson ImmunoResearch, Cambridgeshire, UK), and CAR combinations with anti-CD19(fmc63) scFv were assessed by staining with Protein-L (Biotin-Protein L, GenScript, Piscataway, NJ, USA). In both cases, a Streptavidin-PE antibody (BD Biosciences, Franklin Lakes, NJ, USA) was used as a secondary antibody. In addition, the following antibodies were used in the marker evaluation of cell lines: CD19-PE (BD Biosciences), Ig light chain κ -APC, and Ig light chain λ -PE (Biolegend, San Diego, CA, USA).

T cells were electroporated as described above, and cells were maintained in culture for 18 h. CAR-expressing T cells were then cocultured with the target cells at an E:T ratio of 1:2 for 6 h. The culture medium consists of X-VIVO 15 medium containing brefeldin A (Golgi-Plug, BD Biosciences) and monensin (Golgi Stop, BD Biosciences). Cells were then stained both for extracellular and intracellular markers using the PerFix-nc kit following the manufacturer's protocol (Beckman Coulter, Indianapolis, IN, USA). The following antibodies were used during the staining protocol: CD4-BV421 (Biolegend), CD8-PeCy7, IFN γ -FITC (eBiosciences, Thermo Fisher), TNF α -PE (BD Biosciences, USA). Cells were acquired using a BD FACSCanto flow cytometer, and the data were analyzed by Flow Jo software (Treestar Inc, Ashland, OH, USA).

Bioluminescence cytotoxic assay

The protocol was described in detail (37). In brief, luciferase-expressing target cells were transferred to a white round-bottomed 96-well plate in the presence of Xenolight D-Luciferin (75 μ g/ml; Perkin Elmer, Oslo, Norway). CAR-expressing T cells were subsequently added in the mix, and cells were cultured in an incubator (37 °C in 5% CO₂) for the duration of the assay. When indicated, additional supplements such as sIgG and serum were added in the CAR-expressing T cell mix. Luminescence was monitored at every time point by a luminometer (Victor Multilabel Plate Reader, Perkin Elmer) as relative light units (RLUs). For each assay, one group of target cells was cultured alone to determine baseline lysis and another group was cultured in 1% Triton X-100 (Sigma-Aldrich) to determine the maximum lysis. Percentage lysis was calculated with the following equation: % specific lysis = 100 \times (spontaneous cell death RLU - sample RLU)/(spontaneous death RLU - maximal killing RLU).

ZAP-70 phosphorylation

Glass slides (Ibidi, Germany) were washed with boiling piranha solution (70% of pure sulfuric acid with 30% of a 30% hydrogen peroxide solution) for 30 min. After intensive washing with PBS, glass slides were functionalized with 5 μ g/ml

of anti-CD3 (OKT3) (eBiosciences, Thermo Fisher Scientific) or 5 μ g/ml of IgG or 100 μ g/ml of poly-L-lysine for 30 min at room temperature followed by extensive rinsing with PBS + 0.1% of BSA. A total of 8 \times 10⁵ electroporated T cells were washed and resuspended in PBS + 0.1% of BSA, then incubated on each substrate and fixed with 4% of paraformaldehyde during 20 min (Sigma, Germany) after 2, 4, 8, or 16 min after incubation. Cells were washed with PBS + 0.1% of BSA and incubated in 50 mM of NH₄Cl (Sigma, Germany) for 20 min and then rinsed again with PBS + 0.1% of BSA. Cells were permeabilized with 0.5% of Triton-X 100 in PBS + 0.1% of BSA during 15 min before being rinsed with PBS + 0.1% of BSA. Cells were then labeled with 0.1 μ g/ml of Phospho-ZAP70/Syk (Tyr319, Tyr352) Monoclonal Antibody (n3koku5) PE (eBioscience, Thermo Fisher Scientific) in PBS + 0.1% of BSA + 0.05% of saponin (Sigma, Germany) during 1 h. After extensive rinsing with PBS, cells were imaged using a confocal microscope (Zeiss LSM 880 AiryScan) with a 63 \times 1.4 NA objective.

Seahorse mitostress assay

A Seahorse Extracellular Flux (XF96e) Analyzer (Agilent, Santa Clara, CA, USA) was used to measure the oxygen consumption rate, which relates to mitochondria of live lymphocytes cells. Briefly, T cells were electroporated with CD19 CAR, IGK CAR, Kz-19BB CAR, and 19z-KBB. Approximately 16 h after electroporation, cells were seeded onto Cell-Tak (Corning Inc, Corning, NY, USA), anti-CD3 (OKT3) (eBiosciences, Thermo Fisher Scientific), or IgG-coated 96-well XF-PS plates (Agilent, CA, USA). The density of cells was determined to be 1 \times 10⁵ cells/well in Dulbecco's modified Eagle's medium (Thermo Fisher Scientific) XF unbuffered assay media, supplemented with 2 mM sodium pyruvate (Sigma-Aldrich, Norway), 10 mM glucose (Sigma-Aldrich), 2 mM L-glutamine (Thermo Fisher Scientific), adjusted to physiological pH (7.6). The cells were incubated in the absence of CO₂ for 1 h prior to Seahorse measurements (six replicates per experiment). Initially, the cell basal respiration was measured for all groups. Next, oligomycin (Sigma-Aldrich), a potent F1F0 ATPase inhibitor (1 μ M), was added and the resulting oxygen consumption rate was used to derive ATP production by respiration. Then, 1 μ M of carbonyl cyanide p-trifluoromethoxyphenylhydrazon (FCCP) (Sigma-Aldrich) was injected to uncouple the mitochondrial electron transport from ATP synthesis, thus allowing the electron transport chain to function at its maximal rate. The maximal respiration capacity was derived from each group by subtracting non-mitochondrial respiration from the FCCP measurement. Lastly, a mixture of antimycin A (Sigma-Aldrich) and rotenone (Sigma-Aldrich) was added, at 1 μ M, to completely inhibit the electron transport and hence respiration, revealing the non-mitochondrial respiration.

Multicellular tumor spheroid formation

Wells of a 96-well plate were coated with 50 μ l of a 1.5% (w/w) solution of agarose (Corning, New York, NY, USA) in PBS and left to polymerize during 60 min at room temperature. A

Combinatorial IGK-CD19 CAR

total of 1×10^3 BL-41 or Granta-519 cells in 200 μ l of complete RPMI-1640 were then added per well. BL-41 and Granta plates were spun down for 15 min at 1000g and incubated for 1.5 and 9.5 days at 37 °C and 5% CO₂, respectively. For the whole duration of the incubation, the plates were placed in an Incucyte S3 (Essen Bioscience Ltd, Newark, UK) with the following settings: 12 images/day, 1 image/well, 3 channels (phase, green and red). Fifty microliters of a 1:200 solution of Annexin V red (Essen Biosciences, UK) diluted in complete RPMI 1640 was added per well, and the plate was consecutively incubated at 37 °C, 5% CO₂ for 15 min. Mock and IGK CAR-, Kz-19BB-, and CD19 CAR-transduced T cells previously washed and resuspended in complete RPMI-1640 medium were introduced in each well at a final concentration of 1×10^4 cells/ml (50 μ l/well). The plate was then put into an Incucyte S3 with the same settings as described above. Analysis of cytotoxicity was performed using Incucyte software.

Statistical analysis

Student's *t* test, one-way or two-way ANOVA was used in the comparison of two groups. Half-maximal lysis was calculated by nonlinear regression (curve fit) on *GraphPad Prism* (GraphPad Software, Inc).

Data availability

The data that support the findings of this study are available from the corresponding author upon reasonable request.

Acknowledgments—We are grateful to Anne Fåne, Marit Renée Myhre, and Elizabeth Baken for expert technical assistance. We thank the Flow Cytometry Core Facility and The Core Facility for Advanced Light Microscopy at the Institute for Cancer Research, Oslo University Hospital.

Author contributions—S. W., H. K., E. M. I., J. H. M. designed the experiments; H. K., P. D., E. B. S., A. J. performed the experiments; S. W., H. K., E. M. I., P. D. analyzed the experiments; E. B. S., G. K. provided essential material and support; H. K., S. W., E. M. I., and P. D. wrote the text.

Funding and additional information—H. K. was supported by a PhD grant from South-Eastern Norway Regional Health Authority (#2016006). S. W. received grants from the Norwegian Cancer Society (#6829007), the Research Council of Norway (#284983), and an innovation grant from South-Eastern Norway Regional Health Authority (#2018591).

Conflict of interest—The authors declare that they have no conflicts of interest with the contents of this article.

Abbreviations—The abbreviations used are: κ , kappa; λ , lambda; BCR, B cell receptor; BLI, bioluminescence; CAR, chimeric antigen receptor; CD3 ζ , CD3 zeta; EBV, Epstein Barr virus; FCS, fetal calf serum; HS, human serum; Ig, immunoglobulin; IGK, immunoglobulin kappa; IGL, immunoglobulin lambda; IVT, *In vitro* transcribed; RLU, relative light unit; scFv, single chain variable fragment; sIgG, soluble IgG; SR, serum replacement.

References

1. Eshhar, Z., Waks, T., Gross, G., and Schindler, D. G. (1993) Specific activation and targeting of cytotoxic lymphocytes through chimeric single chains consisting of antibody-binding domains and the gamma or zeta subunits of the immunoglobulin and T-cell receptors. *Proc. Natl. Acad. Sci. U. S. A.* **90**, 720–724
2. Maher, J., Brentjens, R. J., Gunset, G., Riviere, I., and Sadelain, M. (2002) Human T-lymphocyte cytotoxicity and proliferation directed by a single chimeric TCRzeta/CD28 receptor. *Nat. Biotechnol.* **20**, 70–75
3. Krause, A., Guo, H. F., Latouche, J. B., Tan, C., Cheung, N. K., and Sadelain, M. (1998) Antigen-dependent CD28 signaling selectively enhances survival and proliferation in genetically modified activated human primary T lymphocytes. *J. Exp. Med.* **188**, 619–626
4. LeBien, T. W., and Tedder, T. F. (2008) B lymphocytes: how they develop and function. *Blood* **112**, 1570–1580
5. Brentjens, R. J., Latouche, J. B., Santos, E., Marti, F., Gong, M. C., Lydane, C., King, P. D., Larson, S., Weiss, M., Riviere, I., and Sadelain, M. (2003) Eradication of systemic B-cell tumors by genetically targeted human T lymphocytes co-stimulated by CD80 and interleukin-15. *Nat. Med.* **9**, 279–286
6. June, C. H., and Sadelain, M. (2018) Chimeric antigen receptor therapy. *N. Engl. J. Med.* **379**, 64–73
7. Paszkiewicz, P. J., Frassle, S. P., Srivastava, S., Sommermeyer, D., Hudecek, M., Drexler, I., Sadelain, M., Liu, L., Jensen, M. C., Riddell, S. R., and Busch, D. H. (2016) Targeted antibody-mediated depletion of murine CD19 CAR T cells permanently reverses B cell aplasia. *J. Clin. Invest.* **126**, 4262–4272
8. Kochenderfer, J. N., Yu, Z., Frasheri, D., Restifo, N. P., and Rosenberg, S. A. (2010) Adoptive transfer of syngeneic T cells transduced with a chimeric antigen receptor that recognizes murine CD19 can eradicate lymphoma and normal B cells. *Blood* **116**, 3875–3886
9. Kalos, M., Levine, B. L., Porter, D. L., Katz, S., Grupp, S. A., Bagg, A., and June, C. H. (2011) T cells with chimeric antigen receptors have potent antitumor effects and can establish memory in patients with advanced leukemia. *Sci. Transl. Med.* **3**, 95ra73
10. Kochenderfer, J. N., Wilson, W. H., Janik, J. E., Dudley, M. E., Stetler-Stevenson, M., Feldman, S. A., Maric, I., Raffeld, M., Nathan, D. A., Lanier, B. J., Morgan, R. A., and Rosenberg, S. A. (2010) Eradication of B-lineage cells and regression of lymphoma in a patient treated with autologous T cells genetically engineered to recognize CD19. *Blood* **116**, 4099–4102
11. Swerdlow, S. H., Campo, E., Pileri, S. A., Harris, N. L., Stein, H., Siebert, R., Advani, R., Ghielmini, M., Salles, G. A., Zelenetz, A. D., and Jaffe, E. S. (2016) The 2016 revision of the World Health Organization classification of lymphoid neoplasms. *Blood* **127**, 2375–2390
12. Vera, J., Savoldo, B., Vigouroux, S., Biagi, E., Pule, M., Rossig, C., Wu, J., Heslop, H. E., Rooney, C. M., Brenner, M. K., and Dotti, G. (2006) T lymphocytes redirected against the kappa light chain of human immunoglobulin efficiently kill mature B lymphocyte-derived malignant cells. *Blood* **108**, 3890–3897
13. Vettermann, C., and Schlissel, M. S. (2010) Allelic exclusion of immunoglobulin genes: models and mechanisms. *Immunol. Rev.* **237**, 22–42
14. Zegers, B. J., Maertzdorf, W. J., Van Loghem, E., Mul, N. A., Stoop, J. W., Van Der Laag, J., Vossen, J. J., and Ballieux, R. E. (1976) Kappa-chain deficiency. An immunoglobulin disorder. *N. Engl. J. Med.* **294**, 1026–1030
15. Ramos, C. A., Savoldo, B., Torrano, V., Ballard, B., Zhang, H., Dakhova, O., Liu, E., Carrum, G., Kamble, R. T., Gee, A. P., Mei, Z., Wu, M. F., Liu, H., Grilley, B., Rooney, C. M., et al. (2016) Clinical responses with T lymphocytes targeting malignancy-associated kappa light chains. *J. Clin. Invest.* **126**, 2588–2596
16. Kloss, C. C., Condomines, M., Cartellieri, M., Bachmann, M., and Sadelain, M. (2013) Combinatorial antigen recognition with balanced signaling promotes selective tumor eradication by engineered T cells. *Nat. Biotechnol.* **31**, 71–75
17. Rohrs, J. A., Siegler, E. L., Wang, P., and Finley, S. D. (2020) ERK activation in CAR T cells is amplified by CD28-mediated increase in CD3zeta phosphorylation. *iScience* **23**, 101023

18. de Felipe, P., Luke, G. A., Hughes, L. E., Gani, D., Halpin, C., and Ryan, M. D. (2006) E unum pluribus: multiple proteins from a self-processing polyprotein. *Trends Biotechnol.* **24**, 68–75
19. Chang, Z. L., Lorenzini, M. H., Chen, X., Tran, U., Bangayan, N. J., and Chen, Y. Y. (2018) Rewiring T-cell responses to soluble factors with chimeric antigen receptors. *Nat. Chem. Biol.* **14**, 317–324
20. Brudno, J. N., and Kochenderfer, J. N. (2018) Chimeric antigen receptor T-cell therapies for lymphoma. *Nat. Rev. Clin. Oncol.* **15**, 31–46
21. Mullard, A. (2017) FDA approves first CAR T therapy. *Nat. Rev. Drug Discov.* **16**, 669
22. Roberts, Z. J., Better, M., Bot, A., Roberts, M. R., and Ribas, A. (2018) Axicabtagene ciloleucel, a first-in-class CAR T cell therapy for aggressive NHL. *Leuk. Lymphoma* **59**, 1785–1796
23. Schuster, S. J., Bishop, M. R., Tam, C. S., Waller, E. K., Borchmann, P., McGuirk, J. P., Jager, U., Jaglowski, S., Andreadis, C., Westin, J. R., Fleury, I., Bachanova, V., Foley, S. R., Ho, P. J., Mielke, S., *et al.* (2019) Tisagenlecleucel in adult relapsed or refractory diffuse large B-cell lymphoma. *N. Engl. J. Med.* **380**, 45–56
24. Maude, S. L., Laetsch, T. W., Buechner, J., Rives, S., Boyer, M., Bittencourt, H., Bader, P., Verneer, M. R., Stefanski, H. E., Myers, G. D., Qayed, M., De Moerloose, B., Hiramatsu, H., Schlis, K., Davis, K. L., *et al.* (2018) Tisagenlecleucel in children and young adults with B-cell lymphoblastic leukemia. *N. Engl. J. Med.* **378**, 439–448
25. Wagner, T. E., Becraft, J. R., Bodner, K., Teague, B., Zhang, X., Woo, A., Porter, E., Albuquerque, B., Dobosh, B., Andries, O., Sanders, N. N., Beal, J., Densmore, D., Kitada, T., and Weiss, R. (2018) Small-molecule-based regulation of RNA-delivered circuits in mammalian cells. *Nat. Chem. Biol.* **14**, 1043–1050
26. Fry, T. J., Shah, N. N., Orentas, R. J., Stetler-Stevenson, M., Yuan, C. M., Ramakrishna, S., Wolters, P., Martin, S., Delbrook, C., Yates, B., Shalabi, H., Fountaine, T. J., Shern, J. F., Majzner, R. G., Stroncek, D. F., *et al.* (2018) CD22-targeted CAR T cells induce remission in B-ALL that is naive or resistant to CD19-targeted CAR immunotherapy. *Nat. Med.* **24**, 20–28
27. Scarfo, I., Ormhoj, M., Frigault, M. J., Castano, A. P., Lorrey, S., Bouffard, A. A., van Scoyk, A., Rodig, S. J., Shay, A. J., Aster, J. C., Preffer, F. I., Weinstock, D. M., and Maus, M. V. (2018) Anti-CD37 chimeric antigen receptor T cells are active against B- and T-cell lymphomas. *Blood* **132**, 1495–1506
28. Koksai, H., Dillard, P., Josefsson, S. E., Maggadottir, S. M., Pollmann, S., Fane, A., Blaker, Y. N., Beiske, K., Huse, K., Kolstad, A., Holte, H., Kvalheim, G., Smeland, E. B., Myklebust, J. H., Inderberg, E. M., *et al.* (2019) Preclinical development of CD37CAR T-cell therapy for treatment of B-cell lymphoma. *Blood Adv.* **3**, 1230–1243
29. Medvec, A. R., Ecker, C., Kong, H., Winters, E. A., Glover, J., Varela-Rohena, A., and Riley, J. L. (2018) Improved expansion and in vivo function of patient T cells by a serum-free medium. *Mol. Ther. Methods Clin. Dev.* **8**, 65–74
30. Zhang, Z., Jiang, D., Yang, H., He, Z., Liu, X., Qin, W., Li, L., Wang, C., Li, Y., Li, H., Xu, H., Jin, H., and Qian, Q. (2019) Modified CAR T cells targeting membrane-proximal epitope of mesothelin enhances the anti-tumor function against large solid tumor. *Cell Death Dis.* **10**, 476
31. Dillard, P., Koksai, H., Inderberg, E. M., and Walchli, S. (2018) A spheroid killing assay by CAR T cells. *J. Vis. Exp.* <https://doi.org/10.3791/58785>
32. Ghorashian, S., Kramer, A. M., Onuoha, S., Wright, G., Bartram, J., Richardson, R., Albon, S. J., Casanovas-Company, J., Castro, F., Popova, B., Villanueva, K., Yeung, J., Vetharoy, W., Guvenel, A., Wawrzyniecka, P. A., *et al.* (2019) Enhanced CAR T cell expansion and prolonged persistence in pediatric patients with ALL treated with a low-affinity CD19 CAR. *Nat. Med.* **25**, 1408–1414
33. Köksal, H., Baken, E., Warren, D. J., Løset, G. Å., Inderberg, E. M., and Wälchli, S. (2019) Chimeric antigen receptor preparation from hybridoma to T-cell expression. *Antib. Ther.* <https://doi.org/10.1093/abt/tbz007>
34. Eyquem, J., Mansilla-Soto, J., Giavridis, T., van der Stegen, S. J., Hamieh, M., Cunanan, K. M., Odak, A., Gonen, M., and Sadelain, M. (2017) Targeting a CAR to the TRAC locus with CRISPR/Cas9 enhances tumour rejection. *Nature* **543**, 113–117
35. Walchli, S., Løset, G. A., Kumari, S., Johansen, J. N., Yang, W., Sandlie, I., and Olweus, J. (2011) A practical approach to T-cell receptor cloning and expression. *PLoS One* **6**, e27930
36. Loew, R., Heinz, N., Hampf, M., Bujard, H., and Gossen, M. (2010) Improved Tet-responsive promoters with minimized background expression. *BMC Biotechnol.* **10**, 81
37. Walseng, E., Koksai, H., Sektioglu, I. M., Fane, A., Skorstad, G., Kvalheim, G., Gaudernack, G., Inderberg, E. M., and Walchli, S. (2017) A TCR-based chimeric antigen receptor. *Sci. Rep.* **7**, 10713
38. Inderberg, E. M., Walchli, S., Myhre, M. R., Trachsel, S., Almasbak, H., Kvalheim, G., and Gaudernack, G. (2017) T cell therapy targeting a public neoantigen in microsatellite instable colon cancer reduces *in vivo* tumor growth. *Oncoimmunology* **6**, e1302631
39. Almasbak, H., Rian, E., Hoel, H. J., Pule, M., Walchli, S., Kvalheim, G., Gaudernack, G., and Rasmussen, A. M. (2011) Transiently redirected T cells for adoptive transfer. *Cytotherapy* **13**, 629–640